Surface wave effects in the upper ocean and consequences for biological modeling

Johannes Röhrs

Dissertation for the degree philosophiae doctor (PhD)
at the University of Bergen

2014

Dissertation date: 21. March 2014

Abstract

Effects of surface gravity waves on particle transport and currents in the upper ocean are studied using field observations and numerical models. Knowledge on upper ocean particle drift is needed for plankton transport studies, search- and rescue operations and oil drift modelling. Such applications depend on upper ocean currents on time scales from hours up to several months, and surface gravity waves affect the air-sea momentum exchange particularly on these time scales. Objects near the surface are also exposed to the wave-induced Stokes drift, which moves particles in the wave propagation direction at a speed with similar magnitude as the Eulerian current. Surface waves furthermore modify the Eulerian mean currents by momentum release during wave breaking and the dissipation of wave energy into oceanic turbulence.

Measurements of upper ocean currents, surface drifters, and waves were taken during field campaigns in Northern Norway. Ocean currents from acoustic Doppler current profilers, high-frequency (HF) radars and satellite-tracked surface drifters were synthesized with wave measurements to separate the Eulerian currents from the Lagrangian, their difference is the Stokes drift. The contribution of waves to surface drifter velocities and observed HF radar currents was quantified and compared with theoretical concepts from the literature. The surface drifters followed the sum of Eulerian currents and Stokes drift with little wind drag. In contrast to previous assumptions, the observation showed that HF radar-derived currents do not include the Stokes drift. The observations were also used to quantify the momentum and energy fluxes from waves into the ocean during a wind event.

The wave-induced drift of suspended plankton was investigated for the example of Northeast Arctic (NEA) cod eggs. Their physical properties are relatively well known, providing a practical example for biological models that depend on oceanic circulation. A combined ocean circulation model, wave model and particle tracking model is used to model pathways of cod eggs from their spawning grounds towards nursery grounds. The cod eggs are affected by *(i)* the Stokes drift; *(ii)* the wave-induced forcing on Eulerian mean currents; and *(iii)* the turbulent mixing induced by breaking waves. Accounting for wave effects in the model system yields more accurate drift velocities and vertical particle distributions compared with observations. Waves are shown to significantly affect the fate of NEA cod eggs: The Stokes drift causes a shoreward flux of particles and thereby reduces the alongshore transport causing retention of NEA cod eggs and larvae around the spawning grounds. The discussed wave effects generally apply to all plankton in the pelagic layer.

The Stokes drift contributes significantly to the fate of drifting particles in the long term because it exhibits a horizontally more uniform direction than the Eulerian currents. The wave field varies on the scales from the atmospheric forcing, giving better predictability than ocean currents. Including wave effects in models therefore facilitates better forecast skills of surface drift applications.

List of papers

1. **Observation-based evaluation of surface wave effects on currents and trajectory forecasts**
   Johannes Röhrs, Kai Håkon Christensen, Lars Robert Hole, Göran Broström, Magnus Drivdal and Svein Sundby
   *Ocean Dynamics **62**, 1519–1533, 2012*

2. **Wave induced transport and vertical mixing of pelagic eggs and larvae**
   Johannes Röhrs, Kai Håkon Christensen, Frode Vikebø, Svein Sundby, Øyvind Sætra and Göran Broström
   in revision for Limnology and Oceanography

3. **Surface wave measurements using a ship-mounted ultrasonic altimeter**
   Kai Håkon Christensen, Johannes Röhrs, Brian Ward, Ilker Fer, Göran Broström, Øyvind Sætra and Øyvind Breivik
   *Methods in Oceanography **6**, 1–15, 2013*

4. **Comparison of HF radar measurements with Eulerian and Lagrangian surface currents**
   Johannes Röhrs, Ann Kristin Sperrevik, Kai Håkon Christensen, Göran Broström and Øyvind Breivik
   submitted to Journal of Physical Oceanography

Scientific environment

The work in this PhD study has been carried out at the Norwegian Meteorological Institute (MET), Division for Oceanography and Marine Meteorology, Bergen. The "BioWave" project, which this study was a central part of, is a collaboration between MET and the Institute of Marine Research (IMR), Bergen. The IMR played a central role in the involved field work, the numerical modeling and in providing expertise on the biological modeling aspects. The work included three field experiments using the research vessel *R/V Johan Hjort* from the IMR and two supplementary cruises using the coastal supply vessel *NSO Crusader* from the Norwegian Coastal Administration. The scientific investigations were carried out together with the MET Division for Ocean and Ice, Oslo. Further cooperation was established with the Geophysical Institute, University of Bergen, and with the Integrative Oceanography Division at the Sripps Institution of Oceanography in San Diego, California, where I spent 6 weeks during my PhD research.

Acknowledgements

I would like to thank my supervisor Kai H. Christensen for a most motivating guidance into science. I very much enjoyed working with you, finding out how the ocean surface works. I also like to thank my co-supervisors Birgitte Furevik, Lars Robert Hole and Göran Broström for their support and inspiration. Great thanks to Svein Sundby and Frode Vikebø from the IMR, who significantly contributed to my research and helped me to get my PhD finished. I further benefited from working with all collaboration partners in the BioWave and OilWave projects, including Øyvind Sætra, Øyvind Breivik, Magnus Drivdal and Ann Kristin Sperrevik who contributed with discussions and ideas.

Further rewards go to all my colleagues at the *Vervaslinga på Vestlandet* and the *Oseanografi og Maritim Meteorologi* group, I had a good time working with you all! Thanks to Magnar Reistad for providing this work place and for covering my back from administrative and monetary issues! This project has been funded by the Norwegian Research Council, further travel funds were granted by ResClim. Thanks to Dave Checkley for organizing my stay at Scripps.

This path for my life had not been possible without my mother, who explained me the math from early on and fought for my education. Thanks to my father for awaking my interest in the earth. Most importantly, I am thankful to Anniken, who supported me every day and night in any possible way.

Contents

Chapter 1

Introduction and Objectives

The upper ocean, which is well mixed and penetrated by sunlight, is the site for primary production and the subsequent flux of biomass to higher trophic levels. Primary and secondary production (phyto- and zooplankton) in the ocean consists of microscopic and relatively small free-drifting organisms. Even fish plankton that feeds on the zooplankton are still so small that their destiny relies mainly on the motion in the upper layer, i.e. ocean currents and turbulent mixing. The understanding of transport, dispersion, growth and mortality in plankton requires an understanding on the mixed-layer dynamics in the upper ocean and on how the plankton responds to its physical environment by adapting buoyancy and vertical behavior.

In addition to ocean currents, particle transport and dispersion in the upper ocean is also determined by waves-induced drift and the turbulent mixing created by breaking waves. Planktonic life in the pelagic layer critically depends on the balance of dynamic forces acting on them (Gawarkiewicz et al., 2007; Prairie et al., 2012), and waves have frequently been identified as important driver for upper ocean dynamics (Sullivan and McWilliams, 2010).

Surface gravity waves are oscillations in sea surface elevation with wavelengths between 10 cm and 1 km and gravity as restoring force (Phillips, 1977). Such waves are nearly always present on the ocean surface. Stokes (1847) showed that particles exposed to waves experience a net forward motion in wave propagation direction —the Stokes drift. This wave-induced drift acts on any particle near the ocean surface in addition to the drift by underlying mean currents. By definition, the Stokes drift is the difference between the particle-following Lagrangian current and the Eulerian current, which an observer at a fixed position experiences.

Measurements from current meters, as well as numeric ocean models, describe Eulerian current fields and the wave-induced Stokes drift is therefore not included. While it is possible to translate time-varying Eulerian fields from ocean models into Lagrangian trajectories, the Stokes drift is typically neglected because the scale of surface gravity waves is not resolved in common ocean models. Trajectory calculations from ocean models are commonly employed for plankton transport studies, oil spill models and search-and-rescue forecasts. These applications depend on near-surface drift, which is affected by waves.

Surface gravity waves also modify the Eulerian mean currents because the wave field contains momentum and energy. As waves grow, travel over long distances, and decay, they redistribute momentum at the air-sea interface (Weber, 1983). During wave

breaking, energy is released to ocean turbulence (see e.g. Melville and Rapp, 1985; McWilliams et al., 2012). Such wave-current interactions affect particle transport indirectly in addition to the direct action of the Stokes drift.

These wave effects emerge whenever the wave energy balance is in a non-equilibrium. Wind driven waves adopt to changes in atmospheric forcing within hours and long surface gravity waves (swell) exists for several days (Magnusson and Reistad, 1998; Burroughs, 1998). On the same time scales, predictions in operational oceanography and weather forecasting are most applicable. This includes forecasts of sea surface elevation during storm surges (Saetra et al., 2007), drift predictions for search-and-rescue missions and oil spill accidents (Breivik and Allen, 2008; Broström et al., 2011), as well as plankton dispersion studies used for fisheries and aquaculture studies and management (Vikebø et al., 2011; Myksvoll et al., 2012). These applications depend on accurate observation and modelling of upper ocean currents, whose modification by waves is the focus of this study.

Because of the nonlinearities in ocean models, the effect of waves on currents is difficult to distinguish from uncertainties due to chaotic spatial variability. However, the predictability of waves is generally much higher than for currents because waves are forced by the atmosphere. Wave fields also exhibit much larger horizontal scales than Eulerian currents. The use of wave models can therefore increase the predictability of surface drift applications.

While comprehensive theoretical knowledge on waves and their interaction with current has existed for many decades (e.g. Longuet-Higgins, 1953; Sullivan and McWilliams, 2010), the wave affected particle transport has rarely been observed in the field nor in the laboratory. How relevant the wave-induced drift is for realistic applications, e.g. for plankton transport, has yet to be determined.

Objectives

The aim of this study is to better understand **the role of surface gravity waves on upper ocean particle transport and plankton dynamics** , thereby improving ocean monitoring and forecasting. To achieve this, the following goals are targeted:

1. Quantifying the importance of wave-induced drift for realistic particle transport
2. Understanding wave effects on Eulerian ocean currents and turbulence
3. Developing methodology to observe wave effects and to distinguish between Eulerian and Lagrangian observations.

The following tools are used to achieve these goals:

- Observations of waves, ocean surface currents, and fish egg distributions
- Implementation of wave-forcing in an ocean model
- Implementation of Stokes drift and wave-induced mixing in a particle tracking model

Chapter 2

Scientific background

2.1 Stokes drift in surface gravity waves

Plane surface gravity waves, as we consider here, are solutions of the Navier-Stokes equation on length scales long enough that capillary forces of the sea surface are negligible, but shorter than distances on which the Coriolis force deflects currents (Phillips, 1977). Current velocities in surface gravity waves oscillate horizontally and vertically to wave propagation direction (Fig. 2.1). For deep water waves, where water depth exceeds one half of the wavelength, the wave motion decays exponentially with depth.

In an Eulerian description with fixed reference points, the orbital velocity of a linear wave solution conducts closed circles. In contrast, when using a Lagrangian description of the flow field by following a particle, it's trajectory performs non-closed cycloids (Stokes, 1847). Figure 2.1 shows Eulerian current vectors and Lagrangian trajectories in a surface gravity wave.

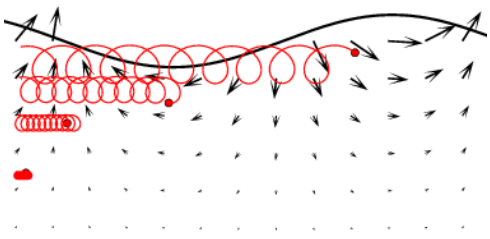

Figure 2.1: Schematic side-view of of the flow field in a surface gravity wave. The sea surface elevation (solid line) describes a transversal wave propagating to the right. Eulerian current velocities at fixed positions (black vectors) perform orbital motions with closed circles, becoming zero when averaged over one wave cycle. Lagrangian particles following the flow describe propagating cycloids (red lines) with a net forward motion, which is the Stokes drift.

This net particle drift in the wave propagation direction — the Stokes drift — arises for two reasons: *(i)* any particle has a forward motion for longer time than the backward motion endures because it moves with the flow while the wave propagates forward; *(ii)* the wave motion decays with depth and a particle is always in the upper part of the orbital motion during its forward moving phase.

The particle motion due to the Stokes drift has already been included into a few Lagrangian trajectory models (e.g. Feng et al., 2011; Broström et al., 2011) by adding the Stokes drift to Eulerian currents from an ocean model, but without considering the wave momentum budget in the ocean model, thus neglecting indirect wave effects on

particle motion by wave-current interactions. The total momentum of the combined ocean and wave system is thereby not conserved (Broström et al., 2008). Other trajectory models use empirical leeway coefficients to describe a drift due to wind and waves, where the Stokes drift is implicitly included through a parameterization by wind speed (Breivik and Allen, 2008). These models are inaccurate when waves and wind are not aligned and during the presence of swell, which is independent of the local wind.

The Stokes drift can be calculated by a numerical wave prediction model that describes the evolution of the wave energy spectrum (Komen et al., 1994). The wave field is discretized in wave frequency and direction, and the growth and attenuation of wave energy by wind and dissipation by friction is modeled for each wave component. Wave energy is exchanged between different wave components by nonlinear wave-wave interactions and advected in space by the group velocity of each component. The Stokes drift is proportional to the wave energy and can be obtained by integrating the wave energy spectrum.

To assess the Stokes drift in field experiments, observations of the two-dimensional wave spectrum are needed. Moored waverider buoys provide an accurate estimation of directional wave spectra, these are mostly used as stationary measurement sites. For measurements during oceanographic cruises, a wave radar system using the ship's nautical radar provides a more flexible system, but these instruments do not observe the high-frequency tail of the spectrum that accounts for a significant part of the Stokes drift.

2.2 Wave forcing on ocean currents

Because waves carry momentum, as manifested by the Stokes drift, they also impact the momentum transfer between the atmosphere and the ocean. During the beginning of a storm, before the wave field is saturated, wave growth consumes momentum fluxes from the atmosphere (Kitaigorodskii et al., 1983). Decaying waves release momentum to the ocean current (Weber, 1983; Longuet-Higgins, 1953) and energy into oceanic turbulence whenever a wave crest breaks (Melville and Rapp, 1985; Gemmrich and Farmer, 2004). The coupling between waves and the mean flow is modified by surfactants, i.e. oil slicks (Christensen and Terrile, 2009).

Wave forcing modifies Eulerian ocean currents during transient wind events and wave breaking (Weber and Melsom, 1993; McWilliams et al., 2012) and through the generation of Langmuir circulation (Craik and Leibovich, 1976; Belcher et al., 2012). In shallow water, wave forcing can accelerate rip and along-shore currents (Michaud et al., 2012; Weber et al., 2009).

The wave forcing during transient wind events is relevant for storm surges (Saetra et al., 2007). For example, in a case where a storm creates waves, a traditional ocean model without wave forcing will use all the momentum flux from the atmosphere to accelerate an ocean current. A coupled wave-ocean model reduces the acceleration of Eulerian ocean currents in the ocean model when waves are created by the storm. The remaining momentum flux from the atmosphere goes into wave momentum, i.e. the Stokes drift increases.

As a brief example for wave-current interaction, we consider an idealized form of the momentum equation, in which waves induce a forcing on the vertically integrated

mean current. Let the fluid velocity in an Eulerian description be given by $v = \bar{v} + \tilde{v}$, where the over-bar denotes mean part and the tilde denotes the wave part. Furthermore, let the surface be given by $z = h + \tilde{\zeta}$ and D is the water depth. In the absence of waves, the volume transport V_E is

$$V_E = \int_{-D}^{h} \bar{v} dz. \tag{2.1}$$

If the total momentum flux from the atmosphere is τ_a, classical Ekman theory yields for the Eulerian volume flux

$$\frac{\partial V_E}{\partial t} + fk \times V_E = \frac{\tau_\mathrm{a}}{\rho}, \tag{2.2}$$

where f is the Coriolis parameter and ρ is the density, here assumed constant. In order to include the effect of the waves, we need to consider the transport all the way up to the surface. We then obtain the *Lagrangian* volume flux V_L, which includes a contribution from Stokes drift in the wave crests (Weber et al., 2006),

$$V_L = \left\langle \int_{-D}^{h+\tilde{\zeta}} v dz \right\rangle = V_E + V_S, \tag{2.3}$$

where the *Stokes transport* V_S is given by

$$V_S = \left\langle \int_{h}^{h+\tilde{\zeta}} \tilde{v} dz \right\rangle. \tag{2.4}$$

If we include the waves, the Ekman dynamics become (Weber et al., 2006)

$$\frac{\partial V_E}{\partial t} + fk \times V_E = F_\mathrm{CS} + \frac{\tau_\mathrm{o}}{\rho}, \tag{2.5}$$

where the contribution from the waves to the forcing of the Eulerian mean flow is given by two distinct mechanisms. The first is the integrated Coriolis-Stokes force:

$$F_\mathrm{CS} = -fk \times V_S, \tag{2.6}$$

and the second is the sea state dependent momentum flux that acts on the Eulerian ocean current, where c_g is the group velocity of surface waves:

$$\frac{\tau_\mathrm{o}}{\rho} = \frac{\tau_\mathrm{a}}{\rho} - \left(\frac{\partial}{\partial t} + c_g \cdot \nabla \right) V_S. \tag{2.7}$$

This last term describes how the momentum flux into the ocean (i.e., the effective surface stress) is modified whenever the waves grow or decay: when the wave grow, the effective surface stress is reduced, when the waves decay, the effective stress is increased compared to the total atmospheric flux τ_a.

The Coriolis-Stokes force (Eq. 2.6) accelerates an Eulerian current perpendicular to the wave motion. In a steady state with no friction, this force creates an Eulerian current that is exactly the opposite of the Stokes drift (Ursell, 1950; Xu and Bowen,

1994). During the evolution of this Eulerian return flow, the effect of the Coriolis-Stokes force is to deflect the Ekman transport, such that the total transport is more than 90 degrees to the right (on the northern hemisphere) of the wind stress (Lewis and Belcher, 2004).

As shown on the example of a vertically integrated momentum equations, the Eulerian current is modified due to the existence of waves at the sea surface. The first study to use this wave forcing in ocean models has been presented by Jenkins (1989), and later works incorporated wave forcing through various wave-current interaction mechanisms (e.g. Ardhuin et al., 2008; Mellor, 2005; Uchiyama et al., 2010).

This study focuses on wave forcing mechanisms that are important in deep water; the Coriolis-Stokes force and the wave dependent stresses introduced in Eq. 2.5. Similar to the forcing of vertically integrated currents, the Coriolis-Stokes force (Eq. 2.6) can be applied to each layer in an ocean circulation model, while the wave dependent stresses (Eq. 2.7) are applied at the surface (Weber et al., 2006). Both wave forcing terms can be calculated with a numerical wave prediction model that describes the evolution of wave energy spectra, as done by Saetra et al. (2007) and in this study (paper II).

2.3 Transport and vertical mixing of cod eggs

The transport and vertical mixing of pelagic fish eggs and larvae is one example for particle transport in the upper ocean. The Northeast Arctic (NEA) cod, which is a fish stock of great commercial value since at least 1000 years, spawns its eggs along the Norwegian coast (Sundby and Bratland, 1987; Sundby and Nakken, 2008). Ocean currents bring the eggs and larvae from the spawning grounds (see Fig. 2.2) into the Barents Sea, which is the nursery ground for juveniles and habitat of the adult fish. The NEA cod is sometimes referred to as Barents Sea cod, and locally as *Skrei*. The detailed knowledge on the physical properties of NEA cod eggs facilitates modeling efforts (e.g. Sundby, 1983; Jung et al., 2012).

Ådlandsvik and Sundby (1994) and Vikebø (2005) modeled the transport of NEA cod eggs from the Norwegian coast to the Barents Sea. While these studies resolved the large-scale transport of eggs from the Norwegian Sea into the Barents Sea, the used ocean circulation models had difficulties to resolve the small-scale transport patterns near distinct spawning grounds along the complex coastline. For example, the models kept eggs from the Vestfjorden bay, where most NEA cod eggs are spawned in nature, inside the bay instead of transporting them northwards. Insufficient model resolution or too inadequate coupling with the atmosphere may have caused this model weakness.

Whenever the ocean current changes with depth, the fate of fish eggs also depends on their vertical position. NEA cod eggs are nearly perfect spheres and slightly buoyant in sea water, they rise towards the ocean surface at a terminal speeds ranging from 0.2 to 1.5 $\mathrm{mm\,s^{-1}}$ depending on egg diameter and buoyancy. For steady state egg concentration profiles, turbulent mixing of eggs balances their buoyancy. The eggs are typically concentrated in the upper 50 m, with an exponentially decaying profile that depends on the ratio between egg buoyancy and turbulent exchange coefficients (Sundby, 1983). During low wind with little turbulent mixing, the eggs are more concentrated towards the surface than during high wind with strong turbulent mixing, as schemati-

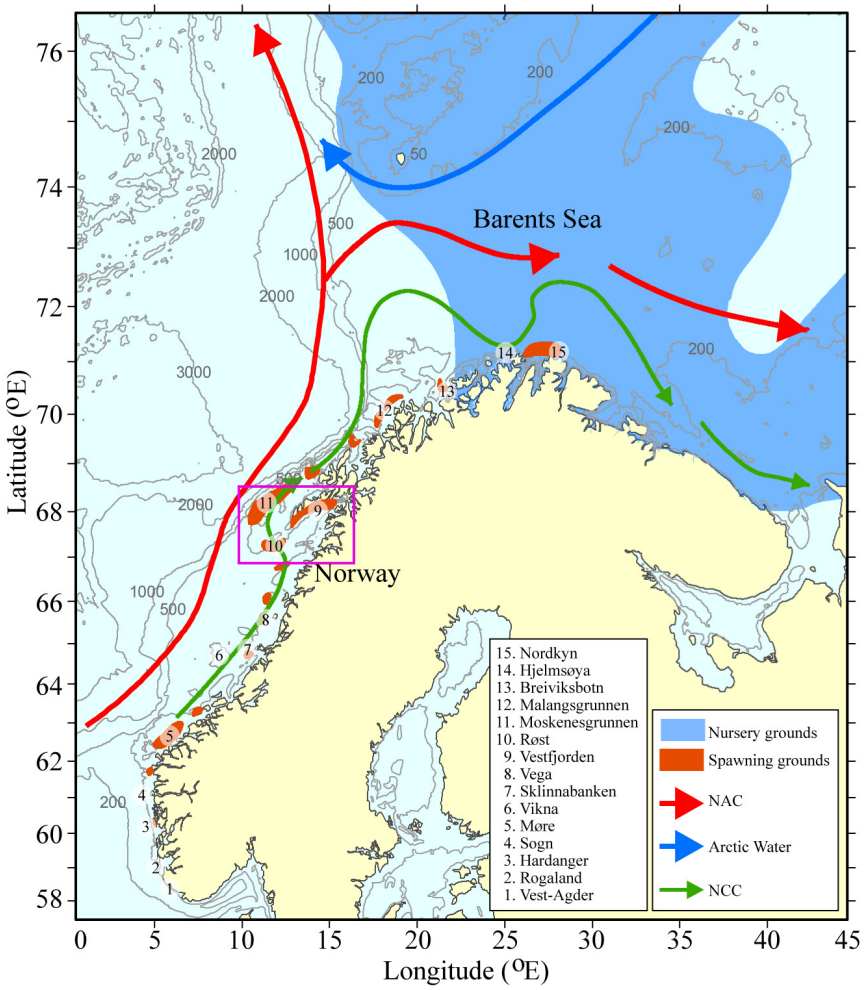

Figure 2.2: Dominating currents in the Norwegian Sea and the Barents Sea. The North Atlantic Current (NAC) transports warm and saline water northwards and the Norwegian coastal current (NCC) transports cold and fresh water from river runoff along the coast towards the Barents Sea. Spawning grounds of the NEA cod are marked as orange patches, the most important spawning ground is in the Vestfjorden bay (patch number 9). The nursery ground of the juveniles is the Barents Sea. A detailed map of the circulation in Vestfjorden, outlined by a pink box, is shown in Fig. 2.4. From Myksvoll et al. (2013).

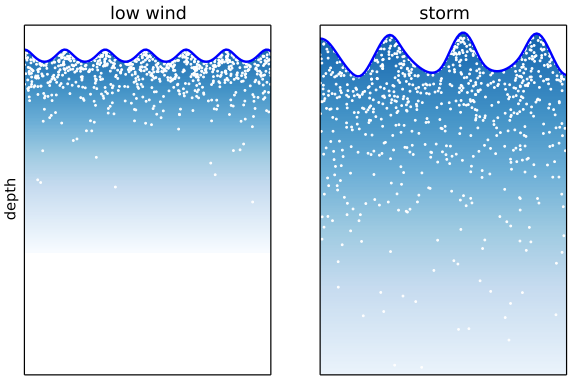

Figure 2.3: Schematic view of cod egg concentrations during low winds with only small waves on the surface and stormy conditions with rough sea state and high waves. The white dots represent individual cod eggs.

cally viewed in Fig. 2.3. Ådlandsvik and Sundby (1994) and Thygesen and Ådlandsvik (2007) developed models for the vertical mixing of cod eggs, which has also been applied to other species (see e.g. Ådlandsvik et al., 2001).

The turbulent mixing of particles can be described with an eddy diffusivity. Sundby (1983) found an empirical eddy diffusivity using wind speed as proxy from observed fish egg concentration profiles. Common ocean models use similar eddy diffusivities for the vertical exchange of momentum, heat and salt. These can be calculated from a conservation budget of turbulent kinetic energy (TKE), often incorporating a second conservation equation, e.g. the for dissipation of TKE or a turbulent length scale (Umlauf and Burchard, 2003). As upper boundary condition for the prognostic TKE equation, the energy flux from dissipation of wave energy can be used (Craig and Banner, 1994) to account for the turbulence induced by breaking waves. While such boundary layer parameterizations are standard components in ocean circulation models, simpler parameterizations based on wind speed are more commonly used in fish egg dispersion studies Curtis et al. (2007).

2.4 Ocean circulation in Vestfjorden

The shelf sea off Lofoten and the Vestfjorden bay — outlined by a pink box in Fig. 2.2 and in more detail in Fig. 2.4 — is the study region in this thesis, using the advantage of existing regional oceanographic knowledge and research infrastructure. The scientific interest and need for monitoring of the NEA cod population has led to the acquirement of much oceanographic knowledge about the Vestfjorden bay.

The circulation in Vestfjorden (Fig. 2.4), studied during repeated field campaigns (e.g. Sundby, 1978; Furnes and Sundby, 1981; Mitchelson-Jacob and Sundby, 2001), is locally driven by winds and externally by tides and adjacent current systems. The North Atlantic current transports warm and salty water along the steep continental shelf slope northwards; it splits north of Lofoten where one branch reaches the Barents Sea while another branch continues northwards (Furevik, 1998). Between the North Atlantic current and the coastline, the Norwegian coastal current transports cold and fresh water originated from river runoff northwards (Sætre, 2007).

The Norwegian coastal current partly enters Vestfjorden on its southeast side along the mainland and exits Vestfjorden on its southwest side along the Lofoten archipelago,

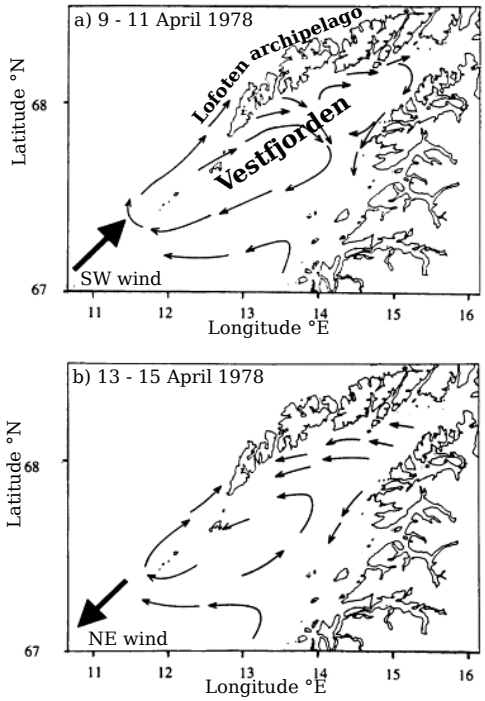

Figure 2.4: Sketches of the circulation of the upper layer in Vestfjorden from oceanographic surveys in April 1978. Furnes and Sundby (1981) identified two major current regimes in Vestfjorden, controlled by southwesterly (a) and northeasterly (b) winds. From Furnes and Sundby (1981).

as shown in Fig. 2.4 (Sundby, 1978). Vestfjorden is separated from the Norwegian Sea by the Lofoten archipelago, a mountain chain with narrow sounds. A rapid exchange of water masses through these sounds by tides is marked by current velocities up to $3\,\mathrm{ms}^{-1}$ (Gjevik et al., 1997).

The dominating wind directions in the western part of Vestfjorden, where most NEA cod eggs are spawned, are southwest and northeast (Sundby, 1982). During southwesterly winds, water masses are pushed into the bay and some outflow occurs on its southeastern side (Fig. 2.4a). Northeasterly winds, which are usually weaker but more steady, set up a cyclonic circulation pattern (Fig. 2.4b) (Furnes and Sundby, 1981) with outflow of water masses along Lofoten, favoring a transport of cod eggs towards the Barents Sea. Ellertsen et al. (1981) showed that these circulation regimes directly affect the fate of cod eggs: During southwesterly winds when water is pushed into the bay, eggs are retained inside Vestfjorden.

Chapter 3

Methodology

This chapter briefly presents the tools used in the paper in th thesis study. Both observations and numerical models are used to investigate the wave forcing on ocean currents and wave-induced particle transport. The observations serve to verify theoretical concepts in the field and to evaluate model results. A model study with an ocean general circulation model combined with a wave model is used to study the effect of waves in a realistic case of plankton transport, which cannot be observed directly.

3.1 Observations of ocean circulation

Three field experiments have been carried out in Vestfjorden and on the shelf sea off Lofoten, the measurements taken during each cruise are summarized in Tab. 3.1. Each of the cruises was simultaneous or directly after the annual stock assessment cruise for the NEA cod in March and April, using the research vessel Johan Hjort of the Institute of Marine Research.

The first cruise in April 2010 was interrupted after only 2 days due to technical problems with the vessel. The most important outcome was a gain in experience used for a better study design in the next year. For the cruise in April 2011, a ship mounted acoustic wave sensor originally developed for the previous cruise was further developed and a new turbulence profiler that could sample directly below the surface was used. The experience with surface drifters from the previous cruise allowed to deploy the drifters with good co-location to other observations.

The cruise in March 2013 was designed with a wider data coverage. High frequency (HF) radars and a mooring with acoustic Doppler current profilers (ADCPs) were deployed a few weeks in advance, such that longer time series of current observations were available for comparison. The main focus of this experiment was to assimilate HF radar currents and hydrography sections into an ocean model (Sperrevik et al., 2014).

To quantify the Stokes drift on drifting objects, Lagrangian current velocities from the surface drifters were compared with Eulerian measurements. The ADCP data provided time series of vertical current profiles, but no information on the horizontal variability of current fields. A comparison with drifter velocities was therefore restricted to fairly short periods when the drifters were close to our moorings.

The HF radars measure area-wide ocean currents along the coast, but measurements are limited to the top one meter of the water column, and are associated with larger uncertainties compared to *in-situ* measurements. HF radars have previously been tested

Table 3.1: Overview of measurements taken during the three cruises in the BioWave project. Satellite tracked drifting buoys that sample the Lagrangian current near the surface were the central tools in these cruises. The iSphere drifters are spherical, half submerged floats with a diameter of 35 cm. The self locating datum marker buoys (SLDMBs) consist of a cross-shaped sail extending from 0.3- to 1.2 m below the surface with small floats at the surface.

April 2010	iSphere surface drifters
	acoustic wave sensor
	tethered micro-structure turbulence profiler
April 2011	iSphere surface drifters
	SLDMB surface drifters
	acoustic wave sensor
	wave rider buoy
	2 moored ADCPs
	autonomous micro-structure turbulence profiler
March 2013	iSphere surface drifters
	SLDMB surface drifters
	pressure sensor (to infer wave spectra)
	3 moored ADCPs
	3 high-frequency (HF) radars

along the Norwegian coast (e.g. Barrick et al., 2012) and may become a powerful tool for operational oceanography through assimilation into ocean models and to provide now-casts of the ocean state. HF radar derived currents are compared with drifter trajectories and ADCP measurements, targeting the question if HF radar currents include a signal from the Stokes drift.

Trajectories from satellite-tracked drifters provide the most accurate description of Lagrangian flow, but these measurements only provide limited data of the flow field along each drifter path. Such drifters are mostly used to validate models (e.g. Liu and Weisberg, 2011) and other measurements such as HF radar currents (e.g. Ohlmann et al., 2007), and to infer dispersion and flow field statistics (LaCasce, 2008). Observations from ADCPs, Lagrangian drifters, and HF radars in the Lofoten region are synthesized in this study to gain understanding on wave-effects on ocean currents and particle transport.

3.2 Modeling of ocean circulation and particle transport

Ocean circulation near the coast of Northern Norway is modeled using a regional setup of the Regional Ocean Modeling System (ROMS) with relatively high horizontal resolution of 800 m to capture the flow along the complex coastline around Lofoten. ROMS solves the Reynolds averaged Navier-Stokes equations to describe and predict the hydrodynamic flow based on the primitive equations. The state variables of the ocean (current velocities, temperature, salinity, sea surface elevation and turbulent quantities) are discretized on a staggered 3-dimensional grid and in time.

Examples of time-averaged surface currents from the model were shown in figure

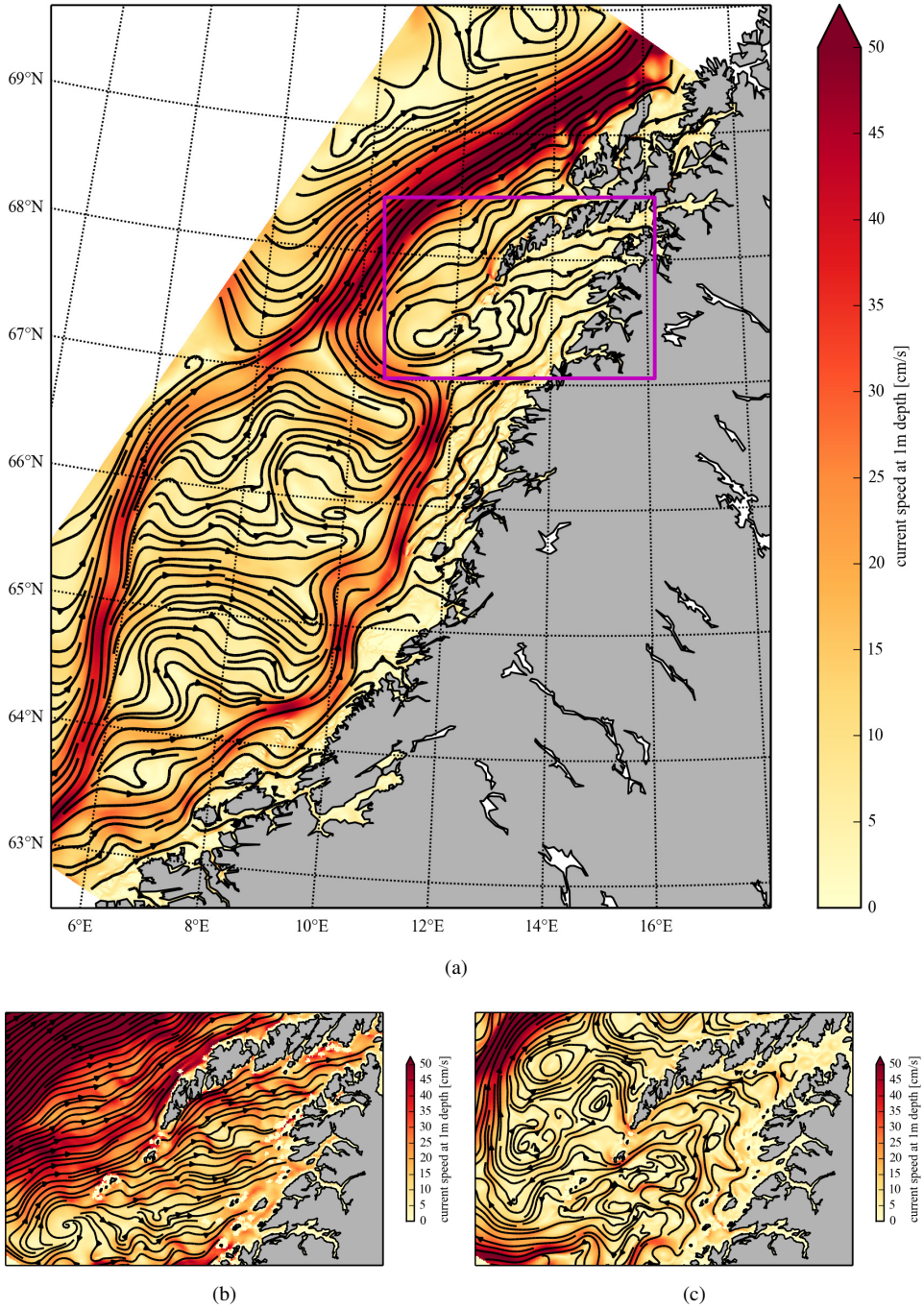

Figure 3.1: Ocean currents at one meter depth from a coastal setup of the ROMS model. a) Average currents from March through April 2011. The model setup covers a 880 km long and 400 km wide domain along the Norwegian coast, stretching from Molde in the south to Finnsnes in the North with a horizontal resolution of 800 m. Further details of the ocean model are given in Paper II of this thesis. b) 24 hour average for Vestfjorden at March 2nd 2011. c) 24 hour average for Vestfjorden at March 14th 2011.

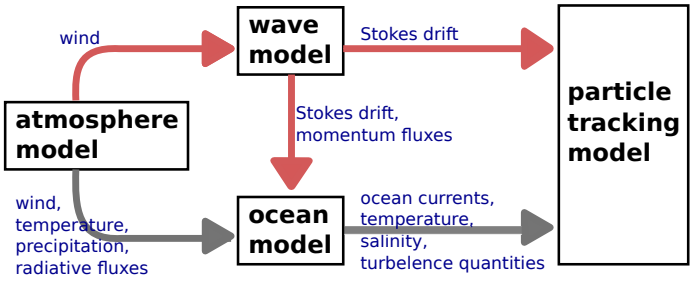

Figure 3.2: Exchange of variables between the components of the used model system. The gray arrows establish a system without wave forcing, used as control run. The red arrows indicate the additional couplings in the wave forced system. For the coupling from the wave model to the ocean model, the Stokes drift is used to compute the Coriolis-Stokes force (Eq. 2.6), and the sea state momentum fluxes are Eq. 2.7.

3.1a. The Norwegian coastal current near the shoreline and North Atlantic current on the shelf slope are the dominant features. Fig. 3.1b and c show examples of typical circulation regimes in Vestfjorden for 24 hour averages, which reveal the wind-driven circulation: During southwesterly winds (b), currents in most parts of Vestfjorden, and in particular along Lofoten, are northwards. During northeasterly winds (c), the Norwegian coastal current enters Vestjorden along the mainland and exits near Lofoten, resulting in a cyclonic circulation in Vestfjorden. These results generally agree with the description presented in section 2.4.

The transport of passive tracers representing NEA cod egg and larvae, hereafter called "model eggs", is modeled using a combination of an ocean model, a wave model, and a Lagrangian particle tracking model. The coupling of the various model components is outlined in Fig. 3.2. While the continuous observations of plankton trajectories is practically unfeasible (Gawarkiewicz et al., 2007), a model system can reveal realistic pathways of fish eggs and larvae (Vikebø et al., 2011; Gallego et al., 2007). Fig. 3.3 shows the pathways of model eggs from the Vestjorden bay to the shelf sea outside Lofoten. Each panel focuses on a different release site, highlighted by red patches, showing how the eggs leave the Vestfjorden bay through different passages represented by arrows. Only model eggs released at the outermost site (panel D) follow the general path of the Norwegian coastal current to exit Vestfjorden. Model eggs from the inner three sites (A-C) depend on a transport through the narrow sounds to exit Vestfjorden.

The modeled transport pathways extend the knowledge on the circulation in Vestfjorden and the transport of cod offspring that has been obtained from observations in the past (Furnes and Sundby, 1981; Ellertsen et al., 1981). While several previous modeling studies focused on the large scale transport of cod eggs from the Lofoten region towards the Barents Sea (Ådlandsvik and Sundby, 1994; Vikebø et al., 2007), the higher resolution model used in this study allowed to focus on the local transport in Vestfjorden. Such detailed knowledge is needed to understand fish stock recruitment mechanisms, manage aquaculture farms, and to assess risks from fossil fuel exploitations.

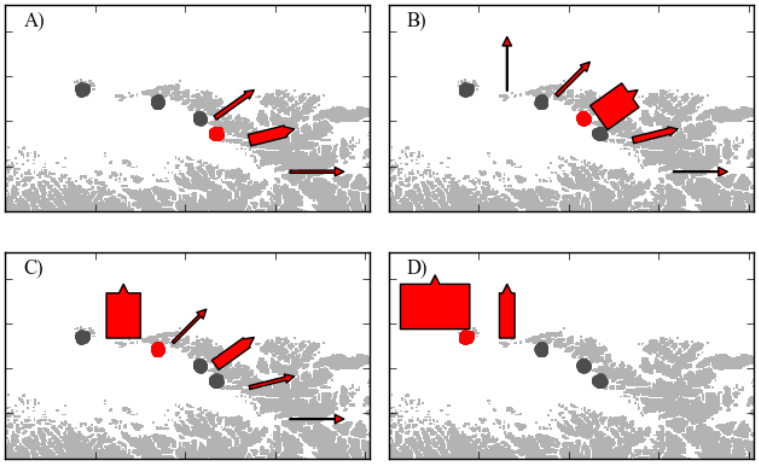

Figure 3.3: Results of the particle tracking model for cod eggs and larvae, details of the model system are given in paper II. Each panel shows which passages are used to exit the Vestfjorden bay, for eggs spawned at the respective site highlighted by a red patch. The width of the arrows indicates the fraction of eggs transported through the respective passage.

3.3 Wave forcing in a regional ocean model

The ocean model ROMS was modified to read forcing data from the numerical wave prediction model WAM. The sea state momentum flux (Eq. 2.7) is calculated by the wave model and applied as surface stress in the ocean model. The Stokes drift is passed to the ocean model as 3-dimensional fields to apply the the Coriolis-Stokes force (Eq. 2.6) to each layer of the ocean model. The variables exchange between the model components is summarized in Fig. 3.2.

As an example on the response of the ocean model to the wave forcing, a storm surge during March 2nd 2011 in is shown in Fig. 3.4. Upper ocean currents at the same day were shown in figure 3.1a. Southeasterly winds pushed water masses into Vestfjorden, raising the sea level in Vestfjorden (Fig. 3.4a). Figure 3.4b shows the effect of wave forcing on this storm surge by displaying the difference between the model run with wave forcing and a control run without wave forcing. The wave field, illustrated by the Stokes drift, is shown in figure 3.4c.

Region A in Fig. 3.4b shows a relative decrease in sea level in the wave-forced model run compared to the control run. The reason is the wave forcing term in Eq. 2.5: growing waves at region C (Fig. 3.4c) effectively reduce the ocean surface stress, which accelerated the northward ocean current causing the storm surge in Vestfjorden.

Region B in Fig. 3.4b shows a relative increase in sea level in the wave-forced model run, caused by the Coriolis-Stokes term in Eq. 2.5. Northward Stokes drift in region D (Fig. 3.4c) cause the acceleration of a westward, wave-induced current through the Coriolis-Stokes force which pushes water masses towards the coast.

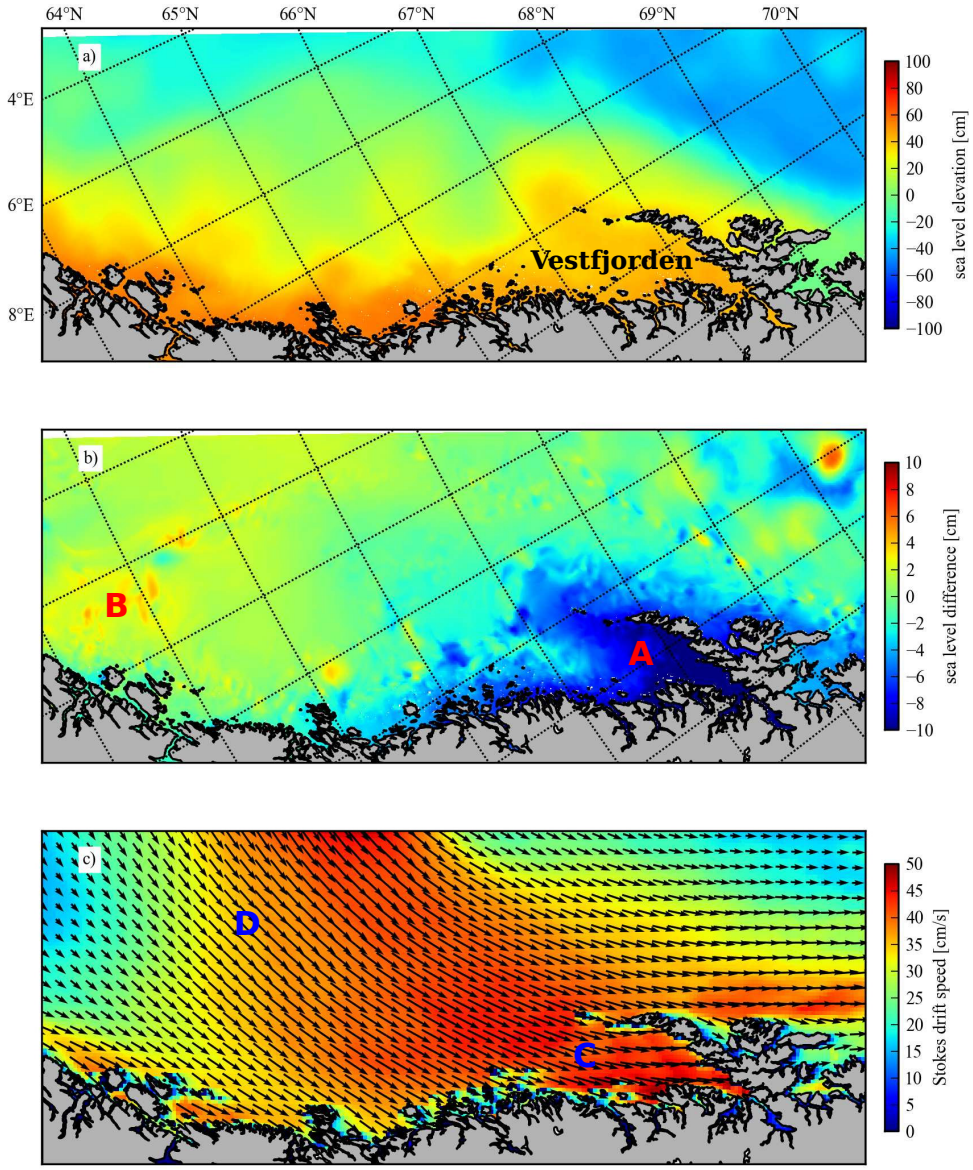

Figure 3.4: Sea surface elevation and the Stokes drift during a storm event on March 2nd 2011, 19:00 CET. a) Sea surface elevation from the ROMS ocean model coupled with an ocean model. b) Difference of sea surface elevation between the model run with wave forcing and a control run without wave forcing. c) Stokes drift velocities from the WAM wave model.

Chapter 4

Summary of Results and Perspectives

The papers included in this thesis investigate the Stokes drift contribution in various short-term, upper ocean forecast and monitoring applications:

- Paper I quantifies the Stokes drift contribution to the transport of surface drifters, compared with Eulerian currents and wind drag.
- Paper II quantifies the Stokes drift contribution and wave-induced forcing to plankton transport for the example of cod eggs.
- Paper III presents a new method to collect wave measurements from ships.
- Paper IV addresses whether or not the Stokes drift is contained within the currents measured by HF radars.

The results of these papers are summarized in this chapter with respect to the objectives defined on page 2.

4.1 Quantification of wave-induced drift for realistic particle transport

Paper I and II quantify the contribution of surface waves to particle drift for two examples: Surface drifters and plankton. The drifters (paper I) allowed to directly observe the impact of waves, wind and current on a floating object as they are remotely traceable.

The iSphere drifters (half-submerged spheres) followed the sum of Eulerian currents, the surface Stokes drift and some wind drag. The effect of the wind drag on this drifter type is up to 50% of the Stokes drift in magnitude, depending on the local wind and wave conditions. Accordingly, this drifter was mostly subject to the large scale atmospheric forcing that sets the wind and wave field. The SLDMB drifters (located at 1 m depth) could not be directly compared with Eulerian current observations, but their velocity statistics implied that this drifter type was mostly affected by the small scale variability of the ocean currents, hence not much affected by wind and waves.

In paper II we explore how the Stokes drift modifies the fate of pelagic particles for the example of cod eggs and larvae. A particle tracking model, which uses currents from an ocean model, was extended to include the Stokes drift from a wave prediction model. The ocean model was also modified to account for the wave-forcing on

the Eulerian ocean currents. Modeled surface drifter velocities are compared with velocities from real surface drifters, showing that drifter velocities are statistically better represented when waves are accounted for in the model.

Modeled trajectories of NEA cod eggs are investigated in paper II. The net effect of the Stokes drift was a shoreward transport of cod eggs. For NEA cod eggs in the Lofoten region, waves concentrated model eggs on average 1.5 km closer to land, which is 20% of their total distance to the coast. This coastal retention reduced the the speed of the egg transport to the Barents Sea. Conclusively, the wave-induced drift of particles accumulated over time can be distinguished from the noise of chaotic particle diffusion.

4.2 Wave effects on ocean currents and turbulence

Eulerian mean currents

In paper I, the momentum flux from waves into the ocean was calculated from measured wave spectra during the field experiment in Vestfjorden, April 2011. During a 12 hour wind event with winds up to $15\,\mathrm{ms}^{-1}$, the effective ocean stress τ_o varied between 80% to 180% of the total atmospheric τ_a stress. Their difference is attributed to momentum uptake and release by the wave field. The Coriolis-Stokes force was up to 80% of the standard Coriolis force during the experiment.

The momentum flux from the wave field to the Eulerian ocean currents and the Coriolis-Stokes force was implemented into the model system used for paper II. These wave-forcing mechanisms, outlined in section 3.3, ensure that momentum is conserved in the combined wave-ocean model system and significantly altered ocean model results (see e.g. Fig. 5 of paper II).

Wave-induced turbulence

The energy flux from breaking waves into oceanic turbulence was calculated from measured wave spectra in paper I. At a wind speed of $15\,\mathrm{ms}^{-1}$ and 2 m significant wave height, this energy flux is up to $6 \cdot 10^{-4} m^3 s^{-3}$ and thereby lower than the energy flux from the atmosphere into waves (Fig. 5 of paper I). The wave field has thus transported energy away from the measurement site, acting to redistribute momentum and energy at the air-sea interface. The study also shows that a parameterization of the TKE flux into the ocean proposed by Craig and Banner (1994) is fairly accurate in this case.

The TKE-flux boundary condition, as used in the ROMS ocean model (Umlauf and Burchard, 2003; Warner et al., 2005) and in paper II, allowed to model TKE dissipation profiles that generally agreed with observations from a micro-structure turbulence profiler. An approach is presented in paper II to use the TKE budget from the ocean model to describe the mixing of cod eggs. Modeled cod egg profiles agree better with observed cod egg profiles when wave breaking is accounted for.

Turbulent mixing reduces the effect of Stokes drift on particle transport, because particles are efficiently mixed down in situations when waves and turbulence are strong. This may be a relevant mechanism to avoid the stranding of pelagic fish eggs during storm events. Wave-induced turbulence and wave-forcing on Eulerian currents should be considered whenever a particle tracking model is extended with the Stokes drift

because the various wave effects partly obliterate each other, and the isolated effect of the Stokes drift is very dominant in some cases.

4.3 Development of methodology to observe surface currents and wave effects

For paper IV, the methods and results of paper I were re-used: The synthesis of ADCP, drifter and wave data showed that the Lagrangian current of the surface drifters is the sum of Eulerian ADCP surface currents and the Stokes drift calculated from wave data. The observation system thus allowed to distinguish between Eulerian and Lagrangian currents; a similar observation system with partly the same instruments was used in a new experiment with HF radars to interpret HF radar derived currents in terms of Stokes drift contribution.

As HF radar currents agree well with Eulerian ADCP currents, and with drifter speed where the Stokes drift has been subtracted, we conclude that HF radars measure the Eulerian current and hence do not include the Stokes drift. The second-order correction to the phase velocity of surface gravity waves, which has previously been suggested to impact HF radar currents (Barrick and Weber, 1977), has only a small contribution compared to the uncertainties of the HF radar current estimates. no conclusion can therefore be made if this correction term applies to HF radar currents. The ADCP data also confirms the theoretical analysis of Stewart and Joy (1974), who show that the HF radar measures currents integrated over the upper meter of the ocean. About 80% of the HF radar signal originated from the upper meter during our experiment.

The need for wave information led us to the develop of a low-cost system to observe wind waves and swell directly from a ship, which is presented in paper III. A combination of an ultrasonic altimeter measuring the distance to sea surface and a motion correction unit that tracks the instruments motion relative to the sea surface was used to measure one-dimensional wave spectra. In practice, the altimeter is efficient at observing short wind waves from the ship's bow, while the motion correction unit measures the ship's response to swell. The resulting wave spectra reproduced significant wave height and wave period obtained from the waverider buoy. This new instrument has already been used to study wave-turbulence interaction (Sutherland et al., 2013) and air-sea gas exchange (Bell et al., 2013).

4.4 Perspectives

To study particle drift in the upper ocean, the example of cod eggs provides useful datasets for comparison with vertical particle dispersion in the model. More detailed observations of cod eggs profiles with higher vertical resolution could further be used to study turbulence in the upper mixed layer where wave breaking plays an important role and other measurements of turbulence are difficult to obtain.

A shoreward transport of plankton by waves, as demonstrated for NEA cod eggs in this study, should apply in any ocean on earth because the most dominant waves are always directed towards the shore. Surface gravity waves may thereby play a significant

role in marine ecosystem functioning by concentrating biomass towards the coast, as the wave induced drift should apply to all plankton and nutrients near the surface.

The surface drifters used in this study are also used as surrogate for oil spills and objects pertinent to search- and rescue operations. The presented result, that waves determine the fate of such objects, should also apply to these practical applications. Operational models for trajectory forecasts should therefore use wave data in addition to ocean currents.

An accurate prediction of ocean surface currents on spatial scales below the internal Rossby radius, as needed for operational oceanography, remains a challenge. Ocean currents are sensitive to initial and boundary conditions in ocean models, and today's observations do not cover the spatial variability of the ocean, different to observation networks used for atmospheric forecasts. Assimilation of HF radar data may help to solve this issue in the future. In this study, it has not been possible to directly compare modeled ocean currents with observed currents, because the small scale currents are too sensitive to the chaotic behavior of baroclinic eddies. This issue also complicated an interpretation of the wave forcing in the model. Ensemble model systems should be used to evaluate the overall benefit of having a coupled wave-ocean model system.

Different to boundary layers over land or the sea floor, the ocean surface is neither a flat wall nor a solid wall with variable roughness as assumed in many traditional boundary layer parameterizations. Instead, the ocean surface is an interface in motion which frequently gets disrupted by the breaking of steep waves. Yet there are no comprehensive theories that capture the breaking process of waves on the ocean surface. Taking more wave measurements during future field experiments is likely to provide better understanding of upper ocean dynamics and air-sea interaction.

Modifications of the momentum balance at the air-sea interface by waves is relevant at the same time scales to which the wave field changes. On longer time scales, surface gravity waves are a relevant component of the climate system by mediating gas exchanges between the ocean and the atmosphere through air bubble entrainment during wave breaking (Leifer and De Leeuw, 2006). The capability of waves to strengthen inertial oscillations (Hasselmann, 1970) may also affect ocean-atmosphere exchanges on climate-relevant time scales (Jochum et al., 2012).

References

Ardhuin, F., N. Rascle, and K. A. Belibassakis, 2008: Explicit wave-averaged primitive equations using a generalized Lagrangian mean. *Ocean Model*, **20 (1)**, 35–60, doi: 10.1016/j.ocemod.2007.07.001.

Barrick, D., V. Fernandez, M. I. Ferrer, C. Whelan, and Ø. Breivik, 2012: A short-term predictive system for surface currents from a rapidly deployed coastal HF radar network. *Ocean Dynam*, **62**, 725–740, doi:10.1007/s10236-012-0521-0.

Barrick, D. E. and B. L. Weber, 1977: On the nonlinear theory for gravity waves on the ocean's surface. part ii: Interpretation and applications. *J. Phys. Oceanogr.*, **7 (1)**, 11–21, doi:10.1175/1520-0485(1977)007<0011:OTNTFG>2.0.CO;2.

Belcher, S. E., et al., 2012: A global perspective on Langmuir turbulence in the ocean surface boundary layer. *Geophy. Res. Lett.*, **39 (18)**, L18 605, doi:10.1029/2012GL052932.

Bell, T. G., W. De Bruyn, S. D. Miller, B. Ward, K. H. Christensen, and E. S. Saltzman, 2013: Air-sea dimethylsulfide (dms) gas transfer in the north atlantic: evidence for limited interfacial gas exchange at high wind speed. *Atmospheric Chemistry and Physics*, **13 (21)**, 11 073–11 087, doi:10.5194/acp-13-11073-2013.

Breivik, O. and A. A. Allen, 2008: An operational search and rescue model for the Norwegian Sea and the North Sea. *J Marine Syst*, **69 (1-2)**, 99–113, doi:10.1016/j.jmarsys.2007.02.010.

Broström, G., A. Carrasco, L. R. Hole, S. Dick, F. Janssen, J. Mattsson, and S. Berger, 2011: Usefulness of high resolution coastal models for operational oil spill forecast: the "Full City" accident. *Ocean Sci*, **7**, 805–820, doi:10.5194/os-7-805-2011.

Broström, G., K. H. Christensen, and J. E. H. Weber, 2008: A quasi-eulerian, quasi-lagrangian view of surface-wave-induced flow in the ocean. *J. Phys. Oceanogr.*, **38 (5)**, 1122–1130, doi:10.1175/2007JPO3702.1.

Burroughs, L., 1998: *Guide to wave analysis and forecasting*, chap. 4. Wave forecasting by manual methods, 43–56. World Meteorological Organization.

Christensen, K. H. and E. Terrile, 2009: Drift and deformation of oil slicks due to surface waves. *J Fluid Mech*, **620**, 313, doi:10.1017/S0022112008004606.

Craig, P. D. and M. L. Banner, 1994: Modeling wave-enhanced turbulence in the ocean surface layer. *J. Phys. Oceanogr.*, **24 (12)**, 2546–2559, doi:10.1175/1520-0485(1994)024<2546:MWETIT>2.0.CO;2.

Craik, A. D. D. and S. Leibovich, 1976: Rational model for langmuir circulations. *J Fluid Mech*, **73**, 401–426, doi:10.1017/S0022112076001420.

Curtis, K. A., D. M. Checkley, and P. Pepin, 2007: Predicting the vertical profiles of anchovy (Engraulis mordax) and sardine (Sardinops sagax) eggs in the California Current system. *Fish. Oceanogr.*, **16**, 68–84, doi:10.1111/j.1365-2419.2006.00414.x.

Ellertsen, B., G. Furnes, P. Solemdal, and S. Sundby, 1981: Effects of upwelling on the distribution of cod eggs and zooplankton in Vestfjorden. *Proc. from Norwegian Coastal Current Symposium, Geilo, Norway, 9–12 September 1980 (Eds: R. Sætre and M. Mork.) University of Bergen, 1981: 604–628.*

Feng, M., N. Caputi, J. Penn, D. Slawinski, S. de Lestang, E. Weller, and A. Pearce, 2011: Ocean circulation, Stokes drift, and connectivity of western rock lobster (Panulirus cygnus) population. *Can. J. Fish. Aquat. Sci.*, **68 (7)**, 1182–1196, doi:10.1139/f2011-065.

Furevik, T., 1998: On the Atlantic Water Flow in the Nordic Seas: Bifurcation and Variability. Ph.D. thesis, University of Bergen.

Furnes, G. and S. Sundby, 1981: Upwelling and wind induced circulation in vestfjorden. *Proc. from Norwegian Coastal Current Symposium, Geilo, Norway, 9–12 September 1980 (Eds: R. Sætre and M. Mork). University of Bergen 1981: 152–178.*

Gallego, A., E. W. North, and P. Petitgas, 2007: Introduction: status and future of modelling physical-biological interactions during the early life of fishes. *Mar. Ecol. Prog. Ser.*, **347**, 121–126, doi:10.3354/meps06972.

Gawarkiewicz, G., S. Monismith, and J. Largier, 2007: Observing larval transport processes affecting population connectivity. *Oceanography*, **20 (3)**, 40 – 53, doi: 10.5670/oceanog.2007.28.

Gemmrich, J. R. and D. M. Farmer, 2004: Near-surface turbulence in the presence of breaking waves. *J. Phys. Oceanogr.*, **34 (5)**, 1067–1086, doi:10.1175/1520-0485(2004)034<1067:NTITPO>2.0.CO;2.

Gjevik, B., H. Moe, and A. Ommundsen, 1997: Sources of the maelstrom. *Nature*, **388**, 837–838.

Hasselmann, K., 1970: Wave driven inertial oscillations. *Geophysical Fluid Dynamics*, **1 (3-4)**, 463–502, doi:10.1080/03091927009365783.

Jenkins, A. D., 1989: The use of a wave prediction model for driving a near-surface current model. *Ocean Dynam.*, **42**, 133–149, doi:10.1007/BF02226291.

Jochum, M., B. P. Briegleb, G. Danabasoglu, W. G. Large, N. J. Norton, S. R. Jayne, M. H. Alford, and F. O. Bryan, 2012: The impact of oceanic near-inertial waves on climate. *J. Climate*, **26 (9)**, 2833–2844, doi:10.1175/JCLI-D-12-00181.1.

Jung, K.-M., A. Folkvord, O. S. Kjesbu, A. L. Agnalt, A. Thorsen, and S. Sundby, 2012: Egg buoyancy variability in local populations of atlantic cod (gadus morhua). *Marine biology*, **159 (9)**, 1969–1980, doi:10.1007/s00227-012-1984-8.

Kitaigorodskii, S., M. Donelan, J. Lumley, and E. Terray, 1983: Wave-turbulence interactions in the upper ocean. part ii. statistical characteristics of wave and turbulent components of the random velocity field in the marine surface layer. *J. Phys. Oceanogr.*, **13 (11)**, 1988–1999, doi:10.1175/1520-0485(1983)013<1988:WTIITU>2.0.CO;2.

Komen, G. J., L. Cavaleri, M. Doneland, K. Hasselmann, S. Hasselmann, and P. A. E. Janssen, 1994: *Dynamics and modelling of ocean waves*. Cambridge University Press.

LaCasce, J., 2008: Statistics from lagrangian observations. *Prog Oceanogr*, **77**, 1–29, doi: doi:10.1016/j.pocean.2008.02.002.

Leifer, I. and G. De Leeuw, 2006: Bubbles generated from wind-steepened breaking waves: 1. bubble plume bubbles. *J. Geophys. Res. Oceans*, **111 (C6)**, C06 020, doi: 10.1029/2004JC002673.

Lewis, D. and S. Belcher, 2004: Time-dependent, coupled, ekman boundary layer solutions incorporating stokes drift. *Dynam Atmos Oceans*, **37 (4)**, 313–351, doi: 10.1016/j.dynatmoce.2003.11.001.

Liu, Y. and R. H. Weisberg, 2011: Evaluation of trajectory modeling in different dynamic regions using normalized cumulative lagrangian separation. *J. Geophys. Res.*, **116 (C9)**, C09 013–, doi:10.1029/2010JC006837.

Longuet-Higgins, M. S., 1953: Mass transport in water waves. *Phil Trans R Soc*, **245**, 535–581, doi:10.1098/rsta.1953.0006.

Magnusson, A. K. and M. Reistad, 1998: *Guide to wave analysis and forecasting*, chap. Wave generation and Decay, 34–42. World Meteorological Organization.

McWilliams, J. C., E. Huckle, J.-H. Liang, and P. P. Sullivan, 2012: The wavy ekman layer: Langmuir circulations, breaking waves, and reynolds stress. *J. Phys. Oceanogr.*, **42**, 1793–1816, doi:10.1175/JPO-D-12-07.1.

Mellor, G., 2005: Some consequences of the three-dimensional current and surface wave equations. *J Phys Oceanogr*, **35 (11)**, 2291–2298.

Melville, W. and R. J. Rapp, 1985: Momentum flux in breaking waves. *Nature*, **317 (6037)**, 514–516, doi:10.1038/317514a0.

Michaud, H., P. Marsaleix, Y. Leredde, C. Estournel, F. Bourrin, F. Lyard, C. Mayet, and F. Ardhuin, 2012: Three-dimensional modelling of wave-induced current from the surf zone to the inner shelf. *Ocean Sci*, **8 (4)**, 657–681, doi:10.5194/os-8-657-2012.

Mitchelson-Jacob, G. and S. Sundby, 2001: Eddies of Vestfjorden, Norway. *Cont Shelf Res*, **21(16-17)**, 1901–1918, doi:10.1016/S0278-4343(01)00030-9.

Myksvoll, M., A. Sandvik, J. Skardhamar, and S. Sundby, 2012: Importance of high resolution wind forcing on eddy activity and particle dispersion in a Norwegian fjord. *Estuar Coast Shelf S*, **113**, 293–304, doi:10.1016/j.ecss.2012.08.019.

Myksvoll, M. S., K.-M. Jung, J. Albretsen, and S. Sundby, 2013: Modelling dispersal of eggs and quantifying connectivity among norwegian coastal cod subpopulations. *ICES J. Mar. Sci.*, **70**, doi:10.1093/icesjms/fst022.

Ohlmann, C., P. White, L. Washburn, E. Terrill, B. Emery, and M. Otero, 2007: Interpretation of coastal hf radar-derived surface currents with high-resolution drifter data. *J Atmos Ocean Tech*, **24**, 666–680.

Phillips, O. M., 1977: *The dynamics of the upper ocean*, chap. The dynamics of surface waves, 33–98. Cambridge University Press, London.

Prairie, J. C., K. R. Sutherland, K. J. Nickols, and A. M. Kaltenberg, 2012: Biophysical interactions in the plankton: A cross-scale review. *Limnol. Oceanogr. Fluids and Environments*, **2**, 121–145, doi:10.1215/21573689-1964713.

Saetra, Ø., J. Albretsen, and P. A. E. M. Janssen, 2007: Sea-state-dependent momentum fluxes for ocean modeling. *J. Phys. Oceanogr.*, **37 (11)**, 2714–2725, doi:10.1175/2007JPO3582.1.

Sperrevik, A. K., K. H. Christensen, and J. Röhrs, 2014: Constraining slope currents: assimilation of HF radar currents and CTD hydrography using 4D-Var. *manuscript in preparation*.

Stewart, R. H. and J. W. Joy, 1974: HF radio measurements of surface currents. *Deep Sea Res.*, **21**, 1039–1049, doi:10.1016/0011-7471(74)90066-7.

Stokes, G. G., 1847: On the theory of oscillatory waves. *Trans Cambridge Philos Soc*, **8**, 441–473.

Sullivan, P. T. and J. C. McWilliams, 2010: Dynamics of winds and currents coupled to surface waves. *Annu. Rev. Fluid Mech.*, **42**, 19–42, doi:10.1146/annurev-fluid-121108-145541.

Sundby, S., 1978: In/outflow of coastal water in Vestfjorden. *Council Meeting on International Council for the Exploration of the Sea, 1978 (C:51) : 17 s.*

Sundby, S., 1982: Fresh water budget and wind conditions. *Investigations in Vestfjorden 1978*, Fisken og Havet, 1982: 16 s. [In Norwegian, English abstract].

Sundby, S., 1983: A one-dimensional model for the vertical distribution of pelagic fish eggs in the mixed layer. *Deep Sea Res. I*, **30-6**, 645–661, doi:10.1016/0198-0149(83)90042-0.

Sundby, S. and P. Bratland, 1987: Spatial distribution and production of eggs from North-East Arctic cod at the coast of Northern Norway 1983-1985. Report series Fisken og Havet. Tech. rep., Institute of Marine Research, Bergen.

Sundby, S. and O. Nakken, 2008: Spatial shifts in spawning habitats of arcto-norwegian cod related to multidecadal climate oscillations and climate change. *Ices J. Mar. Sci.*, **65 (6)**, 953–962, doi:10.1093/icesjms/fsn085.

Sutherland, G., B. Ward, and K. H. Christensen, 2013: Wave-turbulence scaling in the ocean mixed layer. *Ocean Sci.*, **9 (4)**, 597–608, doi:10.5194/os-9-597-2013.

Sætre, R., 2007: *The Norwegian Coastal Current*. Tapir Academic Press.

Thygesen, U. and B. Ådlandsvik, 2007: Simulating vertical turbulent dispersal with finite volumes and binned random walks. *Mar. Ecol. Prog. Ser.*, **347**, 145–153, doi: 10.3354/meps06975.

Uchiyama, Y., J. McWilliams, and A. Shchepetkin, 2010: Wave-current interaction in an oceanic circulation model with a vortex-force formalism: Application to the surf zone. *Ocean Model.*, **34**, 16–35, doi:10.1016/j.ocemod.2010.04.002.

Umlauf, L. and H. Burchard, 2003: A generic length-scale equation for geophysical turbulence models. *J. Mar. Res.*, **61**, 235–265, doi:10.1357/002224003322005087.

Ursell, F., 1950: On the theoretical form of ocean swell on a rotating earth. *Mon. Not. Roy. Astron. Soc., Geophys. Suppl.*, **6**, 1–8, doi:10.1111/j.1365-246X.1950.tb02968.x.

Vikebø, F., S. Sundby, B. Ådlandsvik, and O. Otterå, 2007: Impacts of a reduced thermohaline circulation on transport and growth of larvae and pelagic juveniles of Arcto-Norwegian cod (Gadus morhua). *Fish. Oceanogr.*, **16 (3)**, 216–228, doi:10.1111/j.1365-2419.2007.00427.x.

Vikebø, F. B., 2005: The Impact of climate on early stages of Arcto-Norwegian cod - a model apprach. Ph.D. thesis, University of Bergen.

Vikebø, F. B., et al., 2011: Real-Time Ichthyoplankton Drift in Northeast Arctic Cod and Norwegian Spring-Spawning Herring. *PLoS ONE*, **6(11)**, e27 367, doi: 10.1371/journal.pone.0027367.

Warner, J. C., C. R. Sherwood, H. G. Arango, and R. P. Signell, 2005: Performance of four turbulence closure models implemented using a generic length scale method. *Ocean Model.*, **8 (1-2)**, 81 – 113, doi:10.1016/j.ocemod.2003.12.003.

Weber, J., G. Broström, and O. Saetra, 2006: Eulerian vs lagrangian approaches to the wave-induced transport in the upper ocean. *J. Phys. Oceanogr.*, **36**, 2106–2118, doi: 10.1175/JPO2951.1.

Weber, J. E., 1983: Steady wind- and wave-induced currents in the open ocean. *J Phys Oceanogr*, **13 (3)**, 524–530, doi:10.1175/1520-0485(1983)013<0524:SWAWIC>2.0.CO;2.

Weber, J. E., K. H. Christensen, and C. Denamiel, 2009: Wave-induced set-up of the mean surface over a sloping beach. *Cont Shelf Res*, **29**, 1448–1453, doi:10.1016/j.csr.2009.03.010.

Weber, J. E. and A. Melsom, 1993: Transient ocean currents induced by wind and growing waves. *J Phys Oceanogr*, **23**, 193–206.

Xu, Z. and A. J. Bowen, 1994: Wave- and wind-driven flow in water of finite depth. *J Phys Oceanogr*, **24**, 1850.

Ådlandsvik, B., S. Coombs, S. Sundby, and G. Temple, 2001: Buoyancy and vertical distribution of eggs and larvae of blue whiting (Micromesistius poutassou): observations and modelling. *Fish Res*, **50**, 59 – 72, doi:10.1016/S0165-7836(00)00242-3.

Ådlandsvik, B. and S. Sundby, 1994: Modelling the transport of cod larvae from the Lofoten area. *ICES mar. Sci. Symp.*, Vol. 198, 379–192.